Spring 2010

Effect of head-neck posture on human discomfort during whole-body vibration

Jonathan DeShaw
University of Iowa

EFFECT OF HEAD-NECK POSTURE ON HUMAN DISCOMFORT DURING WHOLE-BODY VIBRATION

by

Jonathan DeShaw

A thesis submitted in partial fulfillment
of the requirements for the Master of
Science degree in Biomedical Engineering
in the Graduate College of
The University of Iowa

May 2010

Thesis Supervisor: Assistant Professor Salam Rahmatalla

Graduate College
The University of Iowa
Iowa City, Iowa

CERTIFICATE OF APPROVAL

MASTER'S THESIS

This is to certify that the Master's thesis of

Jonathan DeShaw

has been approved by the Examining Committee
for the thesis requirement for the Master of Science
degree in Biomedical Engineering at the May 2010 graduation.

Thesis Committee: _____
Salam Rahmatalla, Thesis Supervisor

_____
Nicole Grosland

_____
Fredric Gerr

_____
Nathan Fethke

_____
David Wilder

ACKNOWLEDGEMENTS

I would like to acknowledge the people in the 3D Bio-Motion research lab at the Center for Computer Aided Design for their help and support with this thesis project. I would like to thank Sultan Sultan and Ting Xia for their help with the lab setup and preparation. I also express my gratitude to John Meusch and Rosalind Smith for their assistance with the motion capture and data analysis utilized in the 3D Bio-Motion research lab. Finally, I would like to give a special thank you to Salam Rahmatalla for providing his expertise and insights into human dynamics and human discomfort.

TABLE OF CONTENTS

LIST OF TABLES

LIST OF FIGURES

LIST OF ABBREVIATIONS

2D:	two dimensional
3D:	three dimensional
A/D:	analog to digital
DC:	direct current
deg:	degree
DOF:	degree of freedom
gal:	gallon
Hz:	hertz
lbs:	pound
$m \cdot s^{-2}$:	meter per second squared
m:	meter
mm:	millimeter
rad:	radian
RMS:	root mean square
s:	second
WBV:	whole body vibration

CHAPTER I

INTRODUCTION

Problem Statement

It is well known that sitting posture is associated with discomfort and a number of musculoskeletal disorders such as low back pain (Adams and Hutton, 1985). The problem becomes more acute in whole-body vibration (WBV) environments, encountered in aircraft, ships, automobiles, farming machinery, construction equipment, army vehicles, and other moving environments (Rahmatalla et al., 2008). Because of the auto industry demands, correlations have been extensively studied between the head and seat vibration in the seated positions. The dynamics of the head-neck system have been shown to be sensitive to different anthropometry, seating postures, vibration direction, and vibration magnitude (Mansfield and Maeda, 2007). Seat manufacturers have made significant strides toward developing seats for equipment that help alleviating the vibration transferring to the lower area of the spine. While this is seen as a positive achievement, it is likely that the increased neck-head motion resulting from these seat designs was overlooked. Further research is required to understand the motion of the head-neck complex of the seated human and the effect of that on human discomfort. Many cervical spine studies have been developed to estimate the response of the head and neck; however, these studies rarely take the head and neck posture into account. The objective of this work is to show the effect of neck-head posture on the subjective reported discomfort in fore-aft whole-body vibration and to compare that with a new predictive musculoskeletal-based discomfort measure.

Literature Survey

In a study by Fard et al. (2001), the angular velocity of the head and the trunk horizontal acceleration of subjects with strapped trunks were recorded from 0.5 to 10 Hz The authors found that the head-neck complex behavior was quasilinear with one dominant resonance frequency between 0.8 and 1.6 Hz and another dominant frequency

between 5 and 6 Hz. Resonance was found with transmissibilities above 1.0 and showed that an amplification of the system occurs when a forcing frequency approaches a natural frequency In a study by Paddan and Griffin (1988) with fore-and-aft vibration, seat-to-head transmissibilities were measured in two postures: one with a rigid seat without a backrest and one with a rigid seat with a backrest. Without the backrest, transmissibilities were the greatest at 2 Hz. The backrest greatly increased head vibration at frequencies above 4 Hz and caused a second peak at 6 to 8 Hz. They noticed that with a backrest, a significant peak in head acceleration occurred, and if the backrest was removed, the peak was removed. They also showed that the backrest had little effect on side-to-side (lateral) motion, unless the person was wearing a harness. However, without a backrest, the transmission of fore-and-aft motion was restricted mainly to the lower frequencies. With the addition of a backrest, the transmissibility greatly increases to the head motion at all frequencies. Considering the human body as a dynamic system, the transmissibility will depend on the frequency and direction of input motion (Paddan and Griffin, 1988).

In addition to a response in the x-direction (fore-and-aft) from a fore-and-aft vibratory input, a cross axis effect motion may take place the z-direction (vertical) (Fritz, 1998). The latter study also found that the vertical vibration also causes movement in the fore-and-aft direction similar to a “whip stick” but with still smaller movement than in the z-direction. Mansfield and Maeda (2007) analyzed data that showed correlations between resonance frequencies in different directions and concluded a significant cross-axis effect occurred. They also showed that three-dimensional vibration studies are important because the apparent mass resonance frequency is a function of the total vibration magnitude in all axes rather than in just one axis.

Numerous studies have been done in regard to the simulation of human exposure to vibration. Many spine models have been developed modeling the body as rigid links connected by joints with given stiffness, damping, and muscle torque characteristics. Some studies indicate that an appropriate model for the head-neck is a double inverted

pendulum with two resonance frequencies (Viviani and Berthoz, 1975; Fard et al., 2001). Viviani and Berthoz (1975) found that the head-neck system behaves as a quasi-linear second order system with two degrees of freedom. They also found that the presence of a secondary maximum in the gain curves of the transfer functions suggests that the rotation of the head is mainly concentrated around two centers of rotation. One limitation of these models is that only mid-sagittal plane angular motion is taken into account and the effects of translational motions are neglected. Because the head-neck complex has seven vertebrae it is expected that there would be more than one resonance frequency. At low frequencies, the neck can be modeled as a one-degree-of-freedom system, but at higher frequencies, a two-degree-of-freedom system is needed (Fard et al., 2001). Fard et al. (2001) used the response function for the head-neck system to fore-and-aft vibration and found two resonance frequencies for the system. Their model, a double inverted pendulum, showed good consistency between experimental and simulated results. Data published by Ewing and Thomas (1972) indicated that one center of rotation for this model is near the atlantooccipital articulation and the second center of rotation is approximately at the C6-C7 vertebrae.

In the human body, movements of the spine are controlled and restricted by the muscles of the trunk and neck (Fritz, 1998). Because the head is a heavy structure, acting like an inverted pendulum, sensory systems such as the eyes, the labyrinths, and the ears are needed for control (Viviani and Berthoz, 1975). These sensory systems can help determine the complex response of the head-neck muscles. When the body is subjected to vibration, the muscles act in a way to minimize the vibratory oscillations; however, this is believed to be the case only below certain frequencies (Fritz, 1998). A study by Fard et al. (2001) confirmed that "the neck muscles can be activated and produce significant voluntary input only in the low frequency range". Viviani and Berthoz (1975) suggest that below certain frequencies, the head-neck complex actively changes the resistive force in an attempt to oppose the varying load or oscillation and indicate that

this can be seen at frequencies less than 2 Hz. Above 2 Hz, it is hypothesized that people use a dynamic strategy with less focus on individual cycles but rather try to use their muscles to minimize the amplitude of occurring oscillations. A study by Mansfield et al. (2006) suggested that muscle tension may play a role in the peaks in the apparent mass due to vibration and may cause an increase in resonance frequency due to a change in the biomechanical response. Additionally, this could indicate that muscle tension is able to partially control the maximum displacement of the upper body in the fore-and-aft direction.

Hypotheses

The objective of this work was to study and demonstrate the difference in human biomechanical response to WBV compared to the reported subjective discomfort when using different neck postures. Four head-neck postures—up, down, to the side, and normal (straight forward) —were investigated.

Paddan and Griffin (1988) noted that variations in the responses of an individual subject may be due mainly to changes in body posture including that of the head. They also noted that the relative changes in positions between segments may alter the transmission of vibration through the body. Based on the study by Paddan and Griffin (1988) and Fard et al. (2001) it is hypothesized that transmission of vibration to the head differs in the studied frequency range (2 to 8 Hz) when people maintain different upper body postures. It is also hypothesized that there is a change in the reported subjective discomfort when an altered head-neck posture is taken, and that change is especially marked in frequency ranges of head-neck resonance.

Greater head-neck accelerations due to vibration cause greater discomfort. This is shown in transmissibility functions where the input is the vibration accelerations and the output is the resulting head accelerations. Also, at higher magnitude vibration inputs, a greater discomfort in all postures should be seen. Finally, a predictive discomfort function will be investigated to predict human discomfort based on motion data.

CHAPTER II

METHODS

Subjects and Procedure

Ten male subjects were used in the study with an average age of 23.1 ± 2.1years, height of 72.5 ± 3.3 inches, and weight of 188.4 ± 32.2 pounds. The head circumference and neck circumference for each subject were also recorded, with an average of 23.1 ± 0.4 and 15.3 ± 0.7 inches, respectively. Subjects reported no prior neck, shoulder, or head injuries nor any neurological conditions.

Written informed consent, as approved by the University of Iowa Institutional Review Board, was obtained prior to testing. Each subject was informed as to what vibrations they would experience in the study, how the motion data were to be collected, and how the data could be used. To maintain anonymity, each subject was given a subject number.

Four head posture combinations were investigated for this experiment: The four head postures included (1) head-up, (2) head-down, (3) head to the side, and (4) normal (a comfortable neutral position where the subjects look straight forward to a screen attached to the wall in front of them). Additional visual scales were located in other directions to help the subjects maintaining their non-neutral postures. Either four or eight vibration sequences (four postures by one or two amplitudes) were used to complete the experiment. Vibration sequences were randomized for each subject and will also be described in greater detail in the following sections.

In order to acquire correct timing and head-neck posture for data collection, the 10 subjects were trained by giving responses to two random vibration sequences. For the head-up, head-down, and head-to-side postures, subjects were instructed to rotate their heads to the maximum range of motion without excessively straining their necks.

Each subject was fitted as firmly as possible with accelerometers and with light reflective motion-capture markers. The subject was strapped to a seat attached rigidly to a motion platform, which will be described in more details in the following sections. The motion platform was used to generate vibration in the fore-and-aft direction at discrete frequencies of 2 to 8 Hz. Each discrete frequency ran for 15 seconds followed by 5-second stationary breaks at two vibration amplitudes of 0.8 $m \cdot s^{-2}$ RMS and 1.15 $m \cdot s^{-2}$ RMS. During the 15 seconds of vibration, the subject was asked to maintain the desired posture for 5 seconds and verbally rate his discomfort. Once the rating had been given, the subject would change their posture to the normal posture (straight forward) and keep that position for the remaining 10 seconds of the ride file. The subject then made a comparison discomfort rating between the 5 seconds in the non-neutral posture and the 10 seconds in the normal posture. The normal posture was used as the baseline, or control, for the experiment. During the subsequent 5-second stationary break, the subject would reorient his head to the given posture and wait for the next vibration signal. For the head-up, head-down, and head-to-side postures, subjects were instructed to rotate their heads to the maximum range of motion without excessively straining their necks as well as to follow the location of the discomfort scales.

Subjective Reported Discomfort Assessment

Subjects verbally reported their head-neck discomfort using the Borg CR-10 scale, as illustrated in Figure 2.1. The Borg CR-10 scale ranges from 0 to 10, with higher values indicating higher relative discomfort. For this experiment subjects were asked to ignore any other discomfort and rate only the discomfort due to the motion in their head-neck region. Four Borg CR-10 scales were located at precise locations to help each subject maintain his head-neck posture. The head-up scale was located on the ceiling of the room and was angled toward the subject for clear view in the head-up posture. The head-down scale was located on the floor of the room and also angled for appropriate viewing in the head-down posture. The scales viewed for the normal posture and the

head-to-side posture were orientated vertically and placed directly in front and directly to the right side of the subject, respectively, and can be seen in Figure 2.2.

Borg CR10 Scale	
0	Nothing at all
0.3	
0.5	Extremely Weak
0.7	
1	Very Weak
1.5	
2	Weak
2.5	
3	Moderate
4	
5	Strong
6	
7	Very Strong
8	
9	
10	Extremely Strong
*	Absolute Maximum

Figure 2.1 – Discomfort scale

Figure 2.2 – Position of the discomfort scales for the head-to-side and normal postures

Motion Platform Setup

Physical Setup

To generate the vibration motion for the experiment, a six-degree-of-freedom, man rated, motion platform was used (Moog-FCS 628-1800 electrical motion system). The system has capabilities of movement in the translational axes of over 0.39 meters, rotational axes of more than 23 degrees, and accurate frequency response of up to 20 Hz. Subjects were strapped to a rigid seat mounted to the base of the Moog motion platform. The seat pan was inclined at a 5-degree angle to horizontal, and the seat back was inclined at a 14-degree angle to vertical. The seat was covered with a soft thin rubber to increase general comfort while maintaining seat rigidity. For each subject, the seat height was adjusted appropriately to be as high as possible on the subject's back without obstructing the view of the C7 vertebra by the seat back. This height allowed the subject's shoulder blades to make complete contact with the backrest. Subjects were strapped snugly to the seatback by use of a neoprene vest with three central straps and two shoulder straps, as shown in Figure 2.3. This was done in an effort to isolate the head-neck response from dampening effects of the middle and lower back. Quick release buckles were included for safety, in case of emergency.

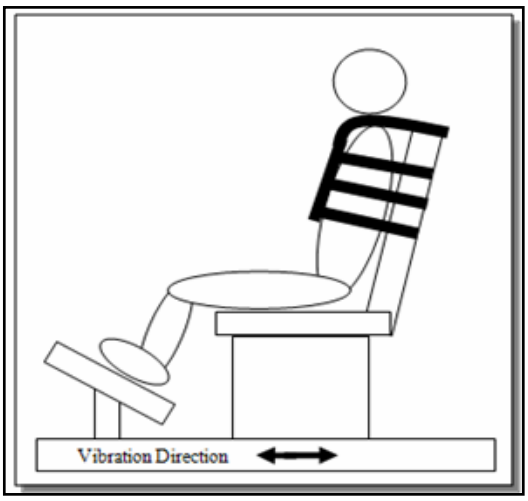

Figure 2.3 – Motion platform setup

Creating Motion Files

Motion files were created using a software package associated with the motion platform (FasTEST Replication). The desired sine wave was 1.15 $m \cdot s^{-2}$ RMS (1.626 $m \cdot s^{-2}$ peak) amplitude and was simulated for each discrete frequency of 2 to 8 Hz in fore-and-aft direction. Because constant accelerations for the input motion were used, larger displacements were required for smaller frequencies.

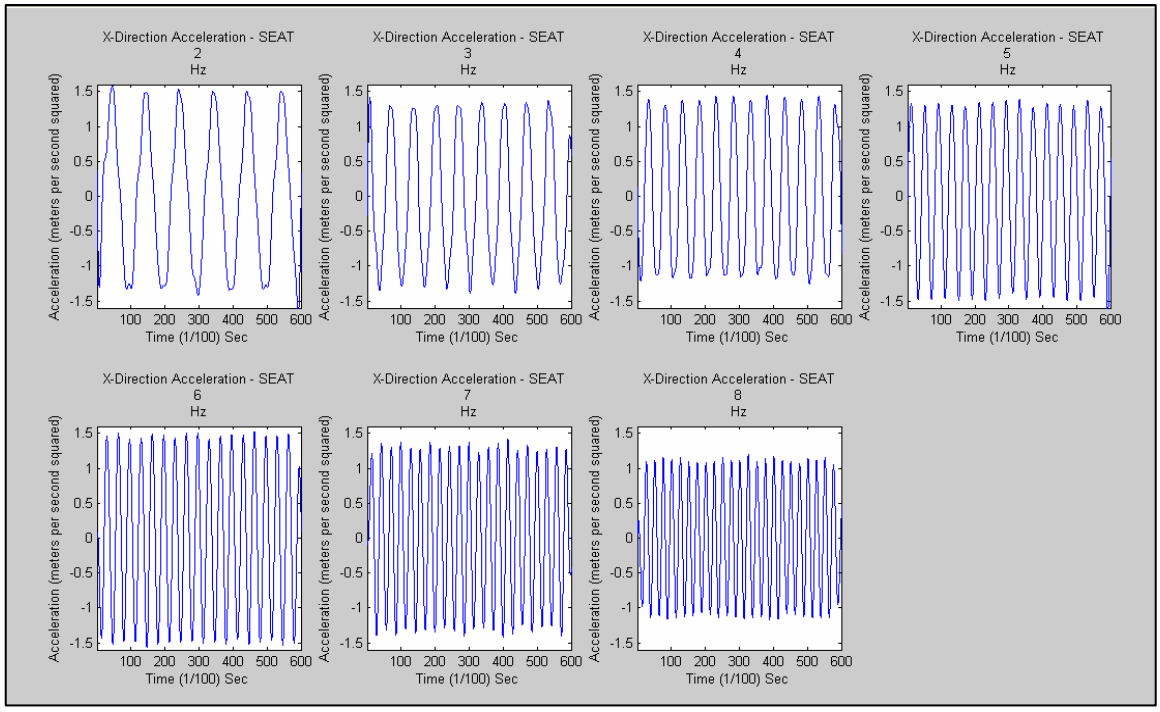

Figure 2.4 – Acceleration of the seat for a three second window for each discrete frequency tested

In the calibration process, the system was calibrated using 15 gallons of water (approximately 125 pounds) to simulate approximate human apparent mass on seat. In order to calibrate the motion a ride file needed to be created and loaded into the system. The ride file consisted of three-dimensional position versus time data. Once the desired motion was sent to the FasTEST program, the Moog system would try to physically

simulate the motion. Three tri-axial accelerometers attached to the motion platform gave feedback to the system for further iterations and corrections. Iterations were repeated until the motion platform response was less than 1% total RMS error of the desired motion. Figure 2.4 shows a three-second window of the measured fore-and-aft accelerations of the motion platform during the experiment for each discrete frequency 2 to 8 Hz. Additional input motions of 0.8 $m \cdot s^{-2}$ RMS (1.131 $m \cdot s^{-2}$ peak) were constructed by the same method and used for later comparison. Each discrete vibration frequency was 15 seconds in length with a 5-second stationary break. The stationary breaks gave each subject time to reset his posture for the upcoming vibration, as described earlier. The total ride time for each trial was 160 seconds, with a total vibration time of 120 seconds.

Randomization

Table 2.1 – Latin-Squares table

A	B	H	C	G	D	F	E
B	C	A	D	H	E	G	F
C	D	B	E	A	F	H	G
D	E	C	F	B	G	A	H
E	F	D	G	C	H	B	A
F	G	E	H	D	A	C	B
G	H	F	A	E	B	D	C
H	A	G	B	F	C	E	D

A Latin-squares table based on the Williams design (1949) was used for randomization of the subjects, postures, amplitudes, and frequencies. Latin-squares tables are used to reduce residual effects in studies with multiple treatments or doses. It was used here to randomize frequency duration effects. A generalized 8 X 8 Latin-squares table is illustrated in Table 2.1. Each posture and amplitude combination was assigned a specific number, 1 through 8, as shown in Table 2.2. Next, the Latin-squares pattern was applied to combine each posture and amplitude combination with each discrete frequency

2 to 8 Hz so that every possible combination was tested. Each subject also started on the subsequent line of the Latin-squares table to further randomize any frequency or duration effects.

Table 2.2 – Eight testing combinations used

PA #	Posture	Amplitude
1	Normal	1.15 $m \cdot s^{-2}$ RMS
2	Normal	0.80 $m \cdot s^{-2}$ RMS
3	Head Down	1.15 $m \cdot s^{-2}$ RMS
4	Head Down	0.80 $m \cdot s^{-2}$ RMS
5	Head to Side	1.15 $m \cdot s^{-2}$ RMS
6	Head to Side	0.80 $m \cdot s^{-2}$ RMS
7	Head Up	1.15 $m \cdot s^{-2}$ RMS
8	Head Up	0.80 $m \cdot s^{-2}$ RMS

Accelerometer Setup

Three DC Crossbow tri-axial accelerometers were used to collect acceleration data for the experiment. The acceleration data were collected at 200 Hz. One accelerometer was placed on the frame of the seat and aligned with the same axes as the motion platform so that a more direct comparison of motion could be made between the simulation ride file and the actual motion. The second accelerometer was located on the C7 vertebra and orientated such that the positive z-direction of the accelerometer was facing posteriorly. The third accelerometer was mounted to the head by use of a rigid halo apparatus worn by the subject and oriented the same as the C7 accelerometer. The halo fits very snugly to each subject's head to minimize any motion artifact. Each accelerometer was adhered to the subjects' skin using medical-grade, double-sided tape, and the head accelerometer was further secured by banded strips of duct tape. While the motion of the subjects are monitored by the motion capture system, the head and seat accelerometers were used in this experiment specifically for comparison with the motion

capture system. A direct comparison between accelerometer data and marker data will be made in the following sections.

Calibration and Data Synchronization

The calibration process of each accelerometer was performed by using the gravity field method. The calibration was done statically by placing the accelerometer on a known flat surface with the active axis up. The voltage was then recorded for a brief time window for each position (turned upward and downward) in all three axes. Because the accelerometers are DC, the voltage readings could be averaged to reach at a maximum and minimum voltage value. The difference between the maximum and minimum voltage readings is then equal to two times that of gravity (9.81 $m \cdot s^{-2}$). Once the calibration of each of the accelerometers is known, a multiplier value can be used quickly to turn the voltage readings into acceleration. In order to ease comparison between the accelerometers and markers, both data sets were synchronized using the Vicon motion capture system data acquisition box. The Vicon system has a 64-channel A/D converter that automatically synchronizes the analog accelerometer to that of the motion capture data. Both the accelerometers and the motion capture data were set for a sampling rate of 200 Hz.

Motion Capture Setup

Marker Protocol

Motion capture technology is becoming increasingly popular in the study of human motion. For this study, a 12-camera Vicon motion capture system was used to acquire the motion of the head, neck, upper trunk, and seat. Data was captured at 200 Hz. Markers were adhered to the skin by medical-grade, double-sided tape. Reflective markers were strategically placed on each subject to capture the motion at the areas of interest. A halo worn by the subjects was fitted with four head markers, Markers were attached to each accelerometer to generate a marker-based local system, which can clearly be seen in the posterior view of Figure 2.5.

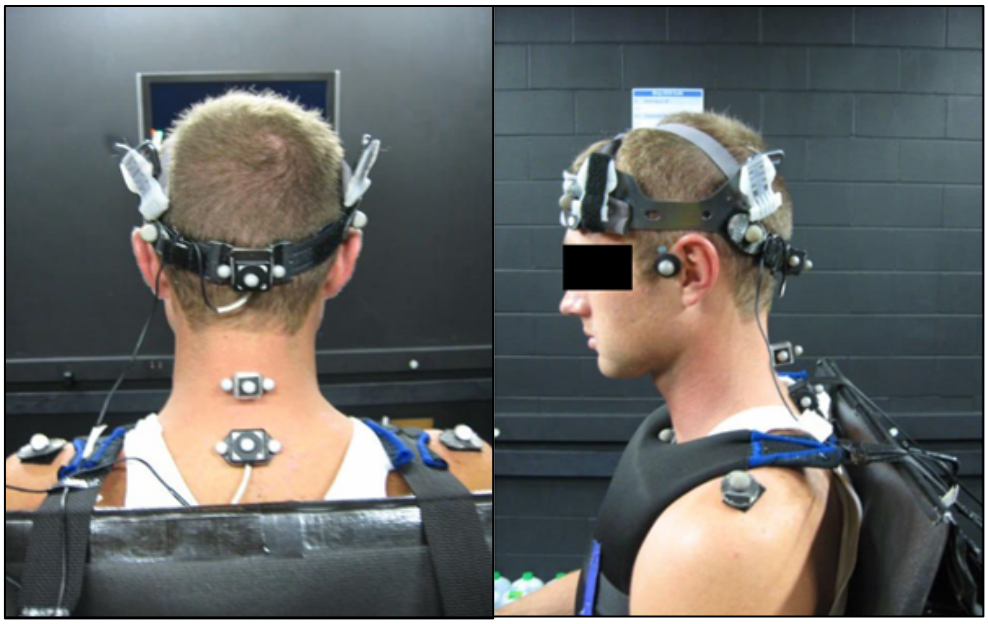

Figure 2.5 – Physical markers placed on each subject for a subject seen in the posterior view (left) and side view (right)

Each local marker-based system can be related to other local marker-based systems and to a global coordinate system. The marker-based local systems are also related to the accelerometer local systems. Three markers fastened to a plastic structure were applied on the spinous process of C3. Another three markers were fitted to an accelerometer and applied on the spinous process of the C7. Additionally, markers were placed on the shoulders, clavicle, and the frame of the seat. Table 2.3 lists the complete marker set for the motion capture.

Table 2.3 - Complete marker set for experiment

NAME	DESCRIPTION
RFHD, LFHD	Placed just superior and lateral to each eyebrow
RBHD, LBHD	Placed on the back of the head, one on each side
RC1, LC1	Placed laterally on the level of C1
C3	Placed on C3 spinous process
C7	Placed on C7 spinous process
CLAV	Placed in the center of the clavicle
RSHO, LSHO	Placed over superior point of the acromion process
RSEAT, LSEAT	Placed on frame of rigid mounted seat

System Calibration

The Vicon system was calibrated using a T-shaped wand and an L-shaped frame which can be seen in Figure 2.6. The frames have reflective markers attached to very specific dimensions recognized by the system. The wand wave is a dynamic calibration and helps the cameras calculate position in space. A good dynamic calibration must be preformed to get accurate results. The L-frame calibration is a static calibration and defines the location of the global coordinate system of the lab.

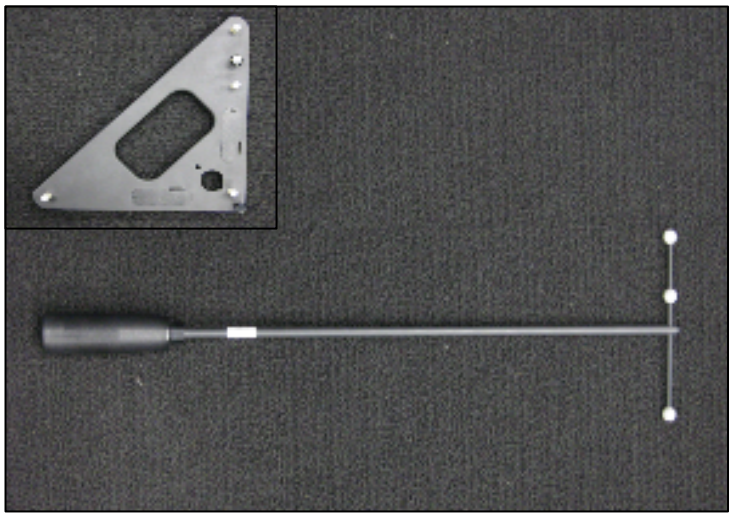

Figure 2.6 – L-frame (upper) and wand (lower) used for Vicon system calibration

Motion Capture Post Processing

Reconstruction of Data and Virtual Points

Vicon iQ 2.0 software was used to post-process the motion capture data. Data were reconstructed where three cameras were needed to see a marker to recognize a point and only two cameras were needed to continue the trajectory of that point in space. A simple marker model set was created using the software, and then the reconstructed data points were color labeled, as shown in Figure 2.7. Because individual markers were useful to capture the motion of points on the skin only, virtual markers were created at

advantageous locations to represent the motion of the joints of the cervical spine. A virtual marker can be created through its relation in space to other markers. An example can be seen in Figure 2.7 where a virtual marker was created in the center of the (C0) using the markers on the halo. Virtual markers were created at the seat, C7, and the center of the head; then the positions with time were exported to a text data file for further data analyses.

The motion capture system uses multiple infrared cameras to triangulate the positions of reflective markers in space. Because of the risk of occlusion (where a marker is hidden from the required number of cameras), redundant markers are used. Redundant markers are additional markers that allow the original marker to be re-created using the motion capture software when occlusion occurs. The markers are attached to bony landmarks on the subject, and the position history is recorded. The system calculates these markers in relation to a given origin in the capture space and gives a global coordinate for each frame.

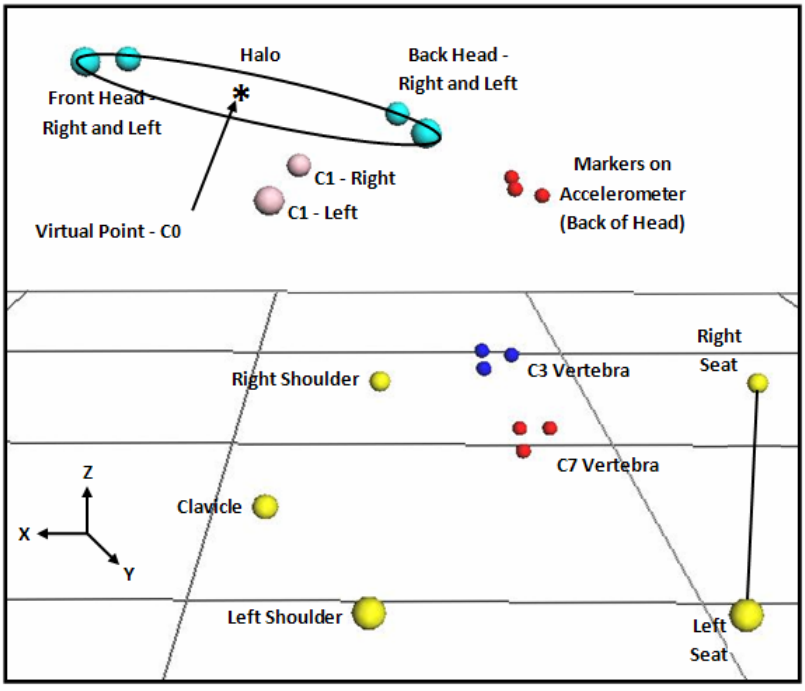

Figure 2.7 – Reconstructed motion capture markers

Validation of Motion Capture Data Using Accelerometers

Accelerometers have been the gold standard to measure whole-body vibration. While accelerometers are reliable, they can be disadvantageous because of the number of accelerometers needed and the need to factor out the gravity acceleration component. In addition, angular and linear displacements calculated from accelerometers using double integration tend to lead to unwanted drift and a lack of a global coordinate system.

Methods of capturing human segment motion have been developed using motion capture systems and have been shown to be reliable. The marker position data can be double differentiated using a five-point central finite difference method to calculate the acceleration of a specific marker or set of markers. A number of filtering and smoothing techniques have been used to obtain useful and realistic acceleration data from the motion capture data (Rahmatalla et al., 2006).

The study by Rahmatalla et al. (2006) showed that acceleration calculated from motion capture position data can successfully be compared to accelerometer data when the marker data is filtered at the correct low-pass frequency. Because data collection in whole-body vibration environments introduces a great deal of noise into the system, an accelerometer is used as a reference for any filtering or smoothing operations to the motion capture data.

To show the quality of the acceleration obtained by differentiating the positions of the motion capture data, a tri-axial accelerometer placed on the back of the head was used to verify the correct low-pass filtering frequency. A program was written in MATLAB to filter the marker position, double differentiate the marker position, and then plot the data versus the accelerometer data. A comparison of the two data sets can be seen in Figure 2.8a, where the marker position was filtered at 12 Hz. Additionally, a tri-axial accelerometer was placed on the rigid seat and aligned with the x-direction so that the gravity component would not need to be removed for comparison. The same procedure was used to generate marker acceleration versus time and was compared to that of the x-

direction from the accelerometer. The data sets can be seen in Figure 2.8b, where the marker position is also filtered at 12 Hz.

(a) (b)

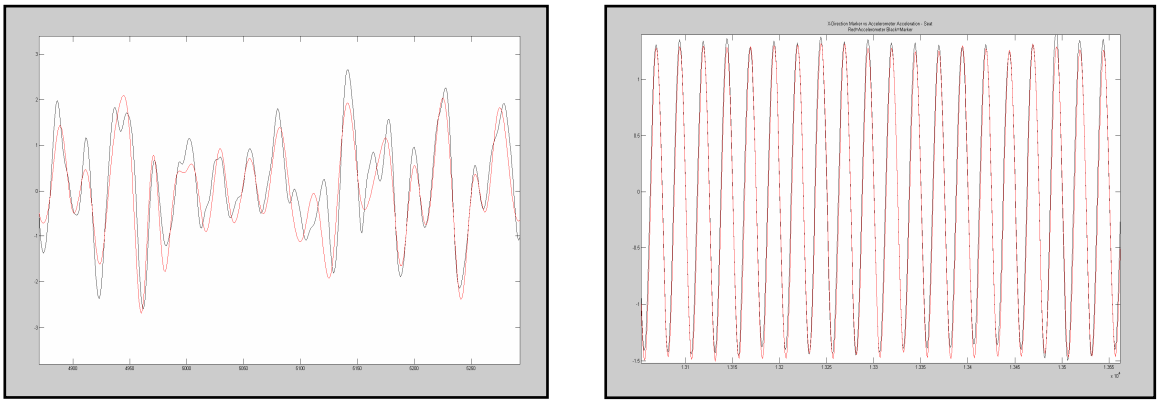

Figure 2.8 – Comparison between calculated marker acceleration data filtered at 12 Hz and accelerometer data for head test (a) and seat test (b). Red is the calculated marker data and black is the accelerometer data

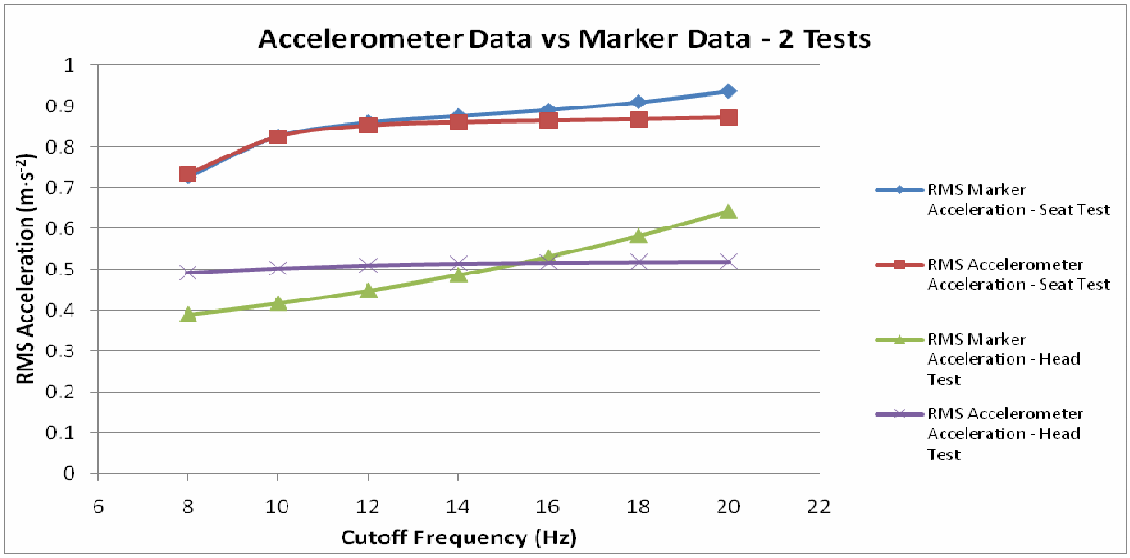

Figure 2.9 – Accelerometer data compared to marker data filtered at cutoff frequencies of 8, 10, 12, 14, 16, 18 and 20 Hz for both head and seat test

To gain insight into what filtering frequency was the most appropriate, a comparison was run for both head and seat tests, and the RMS values of each signal were

evaluated. Low-pass cutoff frequencies of 8, 10, 12, 14, 16, 18 and 20 Hz were used for comparison of the head test and the seat test. The results are presented in Figures 2.8.

As can be seen from the two tests in Figure 2.7 and Figure 2.8, motion capture data can be a very effective tool in evaluating acceleration in vibration environments, especially when post-processed using appropriate filtering and smoothing techniques. The remaining data analysis of this experiment will use the sets of marker data to calculate the positions, velocities, and accelerations of the head-neck system due to vibration.

Calculations

Subjective Reported Discomfort

Because each subject gave an additional response for the normal posture after an altered posture (head down, to-the-side, or up), the normal posture was used as the control. Normal posture is defined as the head in standard anatomical position with the subject facing straight forward. After each gave a discomfort response to an altered head posture response, the subject gave a secondary response in the normal posture to be used as the baseline. Each subject's normal posture responses were then averaged to provide a baseline for normalization. Finally, all subject responses for all postures were divided by each subject's baseline discomfort value. This ensured that while some subjects may have tendencies to give overall higher or lower responses, the general trends can be found. Once subject data were normalized, the 10 subjects' discomfort responses were averaged for each discrete frequency and posture and are presented in the Results section.

Velocity and Acceleration

Once the marker position data is collected and correctly low-pass filtered, it can be used to calculate the velocity and acceleration of the marker by differentiation of the continuous position data. A program in MATLAB was written to use a 5-point central difference method to approximate the differential of the position data to obtain realistic velocity data. The velocity data were then differentiated by the same method to

acceleration data. Caution should be taken when using this method, however, because the ends of the data are not accurate due to the differentiation.

Biomechanical Response

The measure of seat-to-head transmissibility has been the standard for whole-body vibration studies, especially when dealing with seating characteristics or posture (Paddan and Griffin, 1998; Fard et al., 2001; Mansfield, 2004; Viviani and Berthoz, 1975). For random vibrations, the seat-to-head transmissibility is found by taking the cross spectrum of the head acceleration in the frequency domain and dividing it by the auto spectrum of the input vibration and is shown in equation (1) where $G_{io}(f)$ is the cross spectrum and $G_{ii}(f)$ is the auto spectrum.

$$H(f) = \frac{G_{io}(f)}{G_{ii}(f)} \tag{1}$$

Transmissibilities above 1.0 indicate that the output motion is being amplified from the input motion and resonance is occurring. For discrete frequencies, such as in this work, the transmissibility magnitude calculation is much simpler and is equal to the RMS of output acceleration divided by the RMS of input acceleration in the time domain. For this experiment, transmissibility calculations have been performed using the individual-head fore-and-aft, lateral, and vertical directions as the output acceleration component and using the seat fore-and-aft direction acceleration as the input component. Additionally, the total magnitude RMS accelerations for all directions and the angular head velocity were used in the transmissibility calculations.

Predictive Discomfort Function

A predictive function is very useful to predict neck discomfort in response to vibration. A predictive function equation was created to estimate discomfort, based on the idea that a position becomes more uncomfortable when a joint deviates from its neutral position. The predictive discomfort function is presented in this work and applied on the

normal posture only as a proof of concept. For all head-neck positions, joint angles were only considered at one degree of freedom, and the head-neck motion was calculated between the C7 vertebra and the center of the head in the sagittal plane. All side-to-side movements were considered negligible for this pilot test. The predictive function peak discomfort values were averaged, excluding any outliers or other obvious global motion artifact, and an average value was calculated for each discrete frequency. Finally, the predictive discomfort values were normalized by frequency cubed of the input signals and presented in the Results.

CHAPTER III

RESULTS

Subjective Reported Discomfort

Figure 3.1 shows the average reported subjective ratings of 10 subjects based on the Borg CR-10 scale in four different head-neck postures where the data was normalized by each subject's average rated normal posture discomfort. In general, the normal head-neck posture showed a peak at 4 Hz and another peak at approximately 6 Hz. The up, down, and to-the-side postures showed similar trends, with the first peak at 4 Hz, but showed a shift in the second peak to a higher frequency (approximately 7 Hz). After the first peak (4 Hz), the up and the to-the-side postures showed lower discomfort level compared to the normal posture; however, the head-down posture was very sensitive to frequencies higher than 4 Hz and showed a higher discomfort value in that region. The difference between the rated discomfort and the immediate rating of the normal (control) posture can be seen in Figure A.1 in the Appendix A.

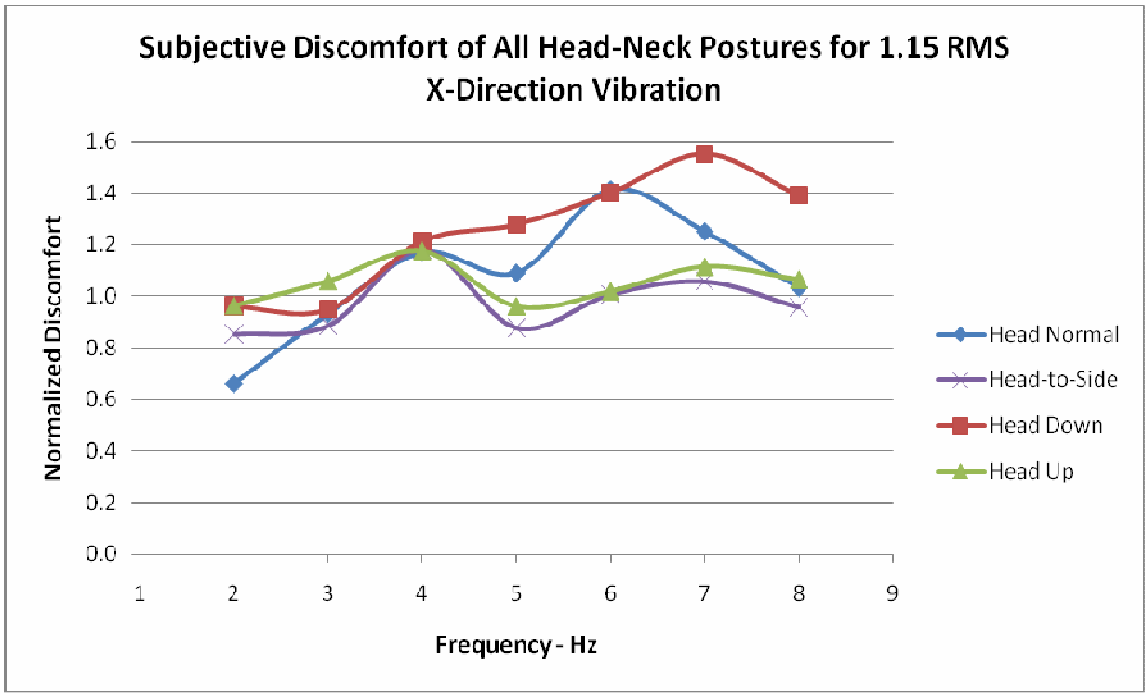

Figure 3.1 –Subjective discomfort ratings from 10 subjects for each head posture

Figure 3.2 shows the difference in average discomfort values between vibration amplitudes of 0.8 and 1.15 $m \cdot s^{-2}$ RMS for all four head postures in the frequency range of 2-8 Hz. The greater vibration amplitude yielded greater subjective discomfort ratings for each posture. The most notable difference between vibration amplitudes within the same posture occurred with the head-down posture. Overall discomfort ratings of the head-to-side posture and head-up posture were slightly lower than the normal posture for the 1.15 $m \cdot s^{-2}$ RMS amplitude; meanwhile, the head-down posture values were the largest with almost twice the reported discomfort. For the lower amplitude vibration, reported discomfort values were very close among head-down, head-up, and normal postures; however, the head-to-side posture discomfort was less.

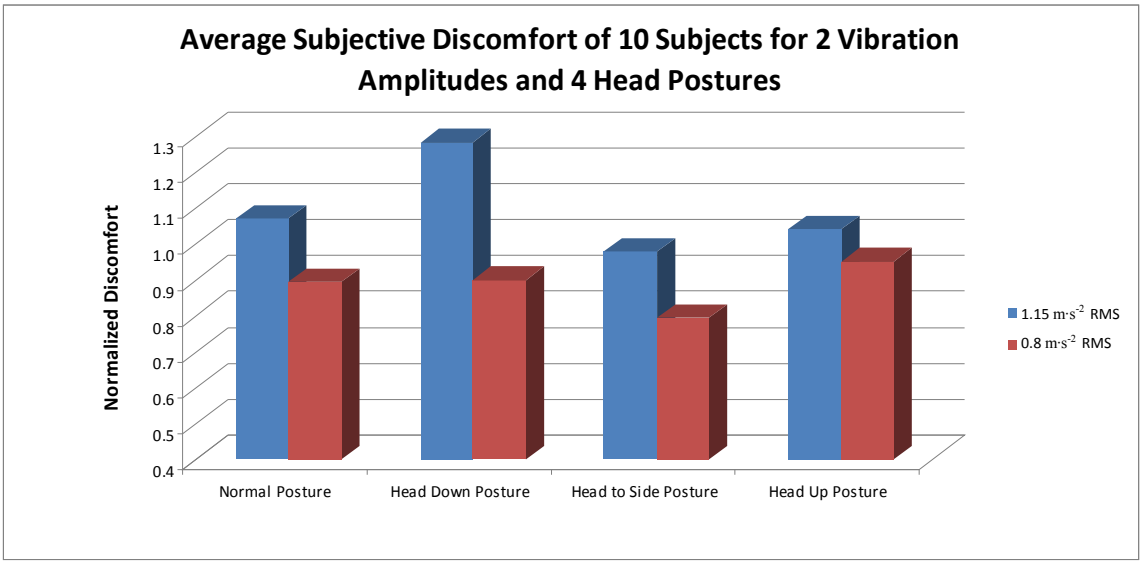

Figure 3.2 – Discomfort between vibration amplitudes and head postures

Biomechanical Response

Figure 3.3 shows the average transmissibility of 10 subjects based on the head position acceleration (C0) in four different head-neck postures. For the transmissibility, the total combined head acceleration magnitudes from the fore-and-aft, lateral, and

vertical motion of the head or the motion in the individual directions were considered as the output, where the acceleration magnitude of the fore-and-aft direction of the seat was the input. Figure 3.3 shows the average of the 10 subjects' specific acceleration component directions by comparing transmissibilities in the fore-and-aft, lateral, and vertical directions, as well as the combined magnitude of all directions. The transmissibility of the fore-an-aft motion of the head is greatest in the low frequency range and can be seen in Figure 3.3a. The head-to-side posture shows a much higher transmissibility in the lateral direction (Figure 3.3b) which makes sense because of head is orientated in the lateral direction in the head-to-side posture. The vertical transmissibility (Figure 3.3c) showed the highest values for the 10 subjects of any direction and indicates a possible head rotational component due to the input vibration.

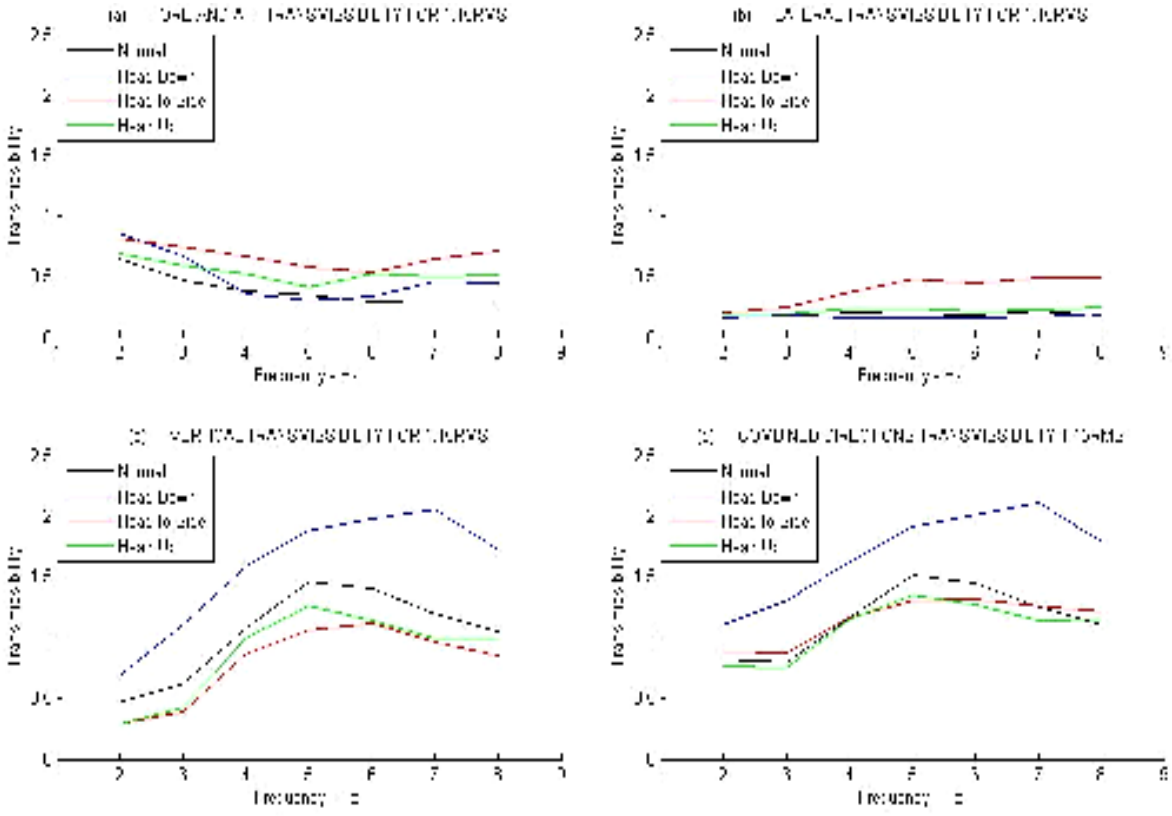

Figure 3.3 – Averaged transmissibility of all 10 subjects for each head posture broken down into individual transmissibility directions

The multidirectional combined transmissibility was calculated by taking the square root of the sum of the squares of each directional RMS acceleration magnitude and then dividing by the RMS acceleration magnitude of the fore-and-aft vibration signal as shown in equation (2).

$$Tx(xyz) = \sqrt{\left(\frac{a_{rms(X)(C0)}}{a_{rms(X)(Seat)}}\right)^2 + \left(\frac{a_{rms(Y)(C0)}}{a_{rms(X)(Seat)}}\right)^2 + \left(\frac{a_{rms(Z)(C0)}}{a_{rms(X)(Seat)}}\right)^2} \quad (2)$$

In general, the multidirectional transmissibility of the normal head-neck posture showed a peak from 5 to 6 Hz as can be seen in Figure 3.3d. The up and the head-to-side postures showed similar trends, with a rounded peak at 5 to 6 Hz, while the down posture showed a peak at around 7 Hz. The head-down posture showed a higher transmissibility at all frequencies. The head-up and head-to-side postures exhibited a similar trend to the normal posture, but were attenuated in the 4 to 7 Hz frequency range.

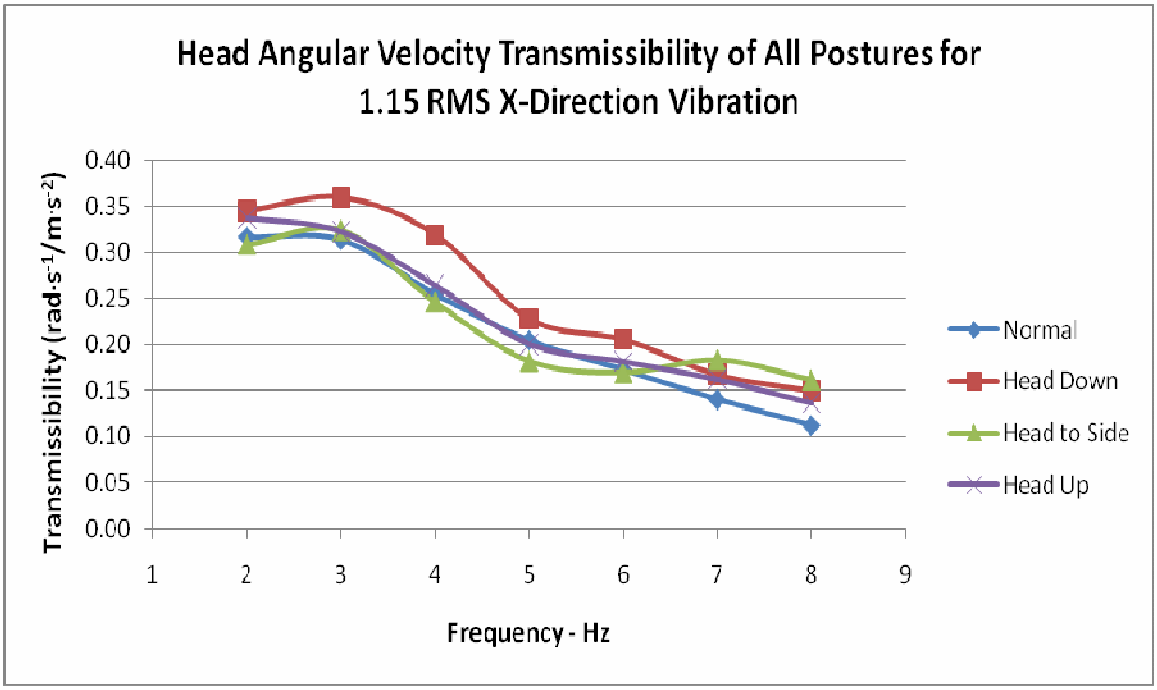

Figure 3.4 – Averaged transmissibility of all 10 subjects for each head posture based on head angular velocity in the pitch direction

Angular velocity transmissibility was also calculated and is presented in Figure 3.4. For this function, the head-neck was considered a 1-DOF system, where output was the angular velocity at the center of the head and the input was the seat acceleration in the x-direction. The transmissibility peaks for all head postures around 2 to 3 Hz, and a second peak can be found in the head-to-side posture at 7 Hz. The head-down posture consistently has a higher transmissibility value throughout the studied range.

Predictive Discomfort Function

Data sets for discomfort, transmissibility, and the predictive discomfort function were normalized by their peaks for comparison and can be seen in Figure 3.6. The predictive function peaks once at around 4 Hz and once again at 6 Hz, which is very similar to the peaks for the subjective reported discomfort. The transmissibility has one peak around 5 Hz, which is much broader than the peaks of the predictive function and subjective reported discomfort.

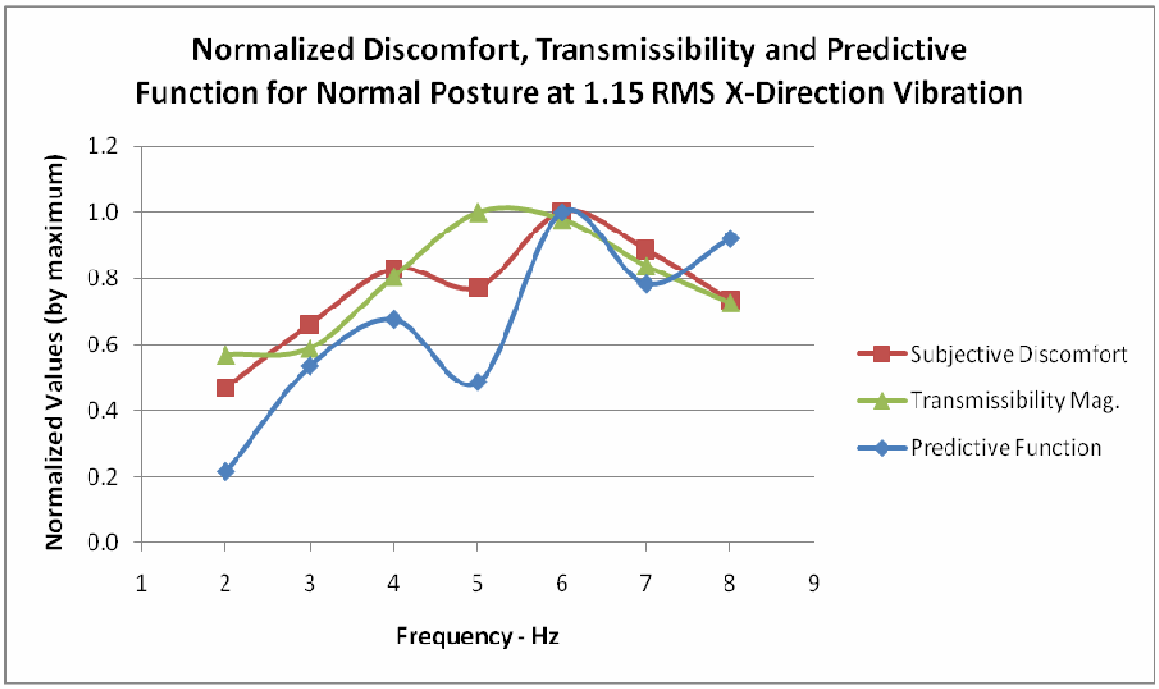

Figure 3.5 – Comparison of normalized discomfort, transmissibility, and predictive function for normal posture

CHAPTER IV

DISCUSSION

Trends in Discomfort Data

The results have shown that the head-neck posture did not affect the location and the magnitude of the discomfort at the low-frequency range, with the first peak at 4 Hz for all postures. However, the head-neck posture plays a more significant role on head-neck motion and discomfort at higher frequencies. This is very clear in Figure 3.1, where the second peak in the discomfort was shifted to a higher peak around 7 Hz for the head-up and head-to-side postures. This might be related to stiffer systems or larger motions with more muscle involvement. For the head-down posture, the magnitude of the discomfort function was higher than for the normal posture. This could be associated with the difficulty of generating more muscle activity in that position to support the head-neck region, resulting in more uncontrolled, uncomfortable motions. As shown in Figure 3.1, the discomfort value for the head-down posture increased steadily after 4 Hz. All postures showed higher discomfort at 2 Hz but the head-up and head-to-side postures showed less discomfort after the first peak at 4 Hz and their magnitudes approach the normal posture around 8 Hz. In these postures, the subjects may be using the major neck-back muscles to alter the biomechanical response. This may create a stiffer system and explain why there is a shift in the second peak in the to-the-side and head-up postures.

Trends in Biomechanical Response

It is known from the literature that subjects supported with a backrest increase their resonance frequency of the head-neck system to the 4 to 6 Hz range (Griffin 1988). Figure 3.3d shows the peak transmissibility of the normal posture to also be in this range. Interestingly, the head-to-side and head-up postures exhibit a similar trend to the normal posture; however, the peak transmissibility is attenuated. In addition, the subject's average transmissibility was lower in this range compared to the normal posture. This suggests that when the head-neck system is stiffened from muscle activity, head

accelerations are attenuated and subjects have less motion in critical frequency ranges. It is clear from Figure 3.3d and Figure 3.4 that the head-down posture has the highest transmissibility for all frequencies. This could be due to the lack of muscle stability in the head-down posture. This trend alone suggests that workers in vibration environments should reduce any head-down postures to avoid unwanted head accelerations and discomfort.

The general trend of angular velocity transmissibility for the normal posture is consistent with that of a study by Fard et al. (2001), but with slightly lesser values and can be found in Figure A.2 of Appendix A. The slightly lesser values were also consistent and could be due to differences in the experimental setup. The extra peak observed in the head-to-side transmissibility may be due to out-of-plane motion generated by a cross-axis effect. The angular head velocity was calculated for only the pitch axis; therefore, the head-to-side posture may not be adequately represented by the angular head transmissibility.

Predictive Discomfort Function

The general trend for the predictive discomfort function seems to match the subjective reported discomfort for the normal posture very well. The predictive function is able to capture relative motion away from the neutral position and relate that to discomfort; however, for higher frequencies a two- degree-of-freedom system will be needed. By normalizing the predictive function by frequency cubed, a greater discomfort weighting is added to higher frequencies and is better at capturing discomfort. In future studies with random vibration, the motion may need to be normalized by frequency cubed first and then calculated with a predictive discomfort function for more accurate results. Also, a pilot investigation has been conducted to evaluate the validity of angular acceleration as part of a predictive discomfort function which shows promising results. Additionally, the rotational acceleration component could be very important for analyzing neck joint forces for discomfort and injury prevention. Finally, the prediction

discomfort function will add value for future human models could be generalized to other joints of the body for discomfort prediction in whole-body vibration.

Future Work

Input Vibration Parameters

The expansion of vibration parameters is necessary in order to gain insight into the complicated response of the head-neck system. Such parameters include frequency spectrum, vibration magnitude and duration, and three-dimensional vibration. A much wider frequency spectrum should be used to capture the full response of the head-neck system to posture change because different low and high frequencies affect local resonances of the neck. The vibration magnitude and duration will play a large role in human discomfort. It may be found that a non-neutral position is more comfortable for a short exposure but over a long exposure or magnitude, it could become much more uncomfortable. Because vibration direction is so important for the response of the head-neck system, all directions should be explored with the ultimate goal to have a three-dimensional simulation and discomfort prediction.

Performance Measures

Additionally, work in the area of performance measures could have large implications in the field of human vibration response. In this age of technology, more and more laptop computers and touch-screen devices are being used in whole-body environments. Recommendations for these devices could be made based upon postural discomfort and performance measures. Visual tracking, touch-screen accuracy, and keyboard-performance studies would also greatly benefit the field of human vibration response.

Predictive Discomfort Function

Finally, future work on a predictive discomfort function is essential in order to get closer to predicting human discomfort mathematically. It would then be possible to mathematically formulate a subject's comfort level based on certain input characteristics.

A multi-degree-of-freedom function would have to be developed, however, in order to capture the complex motion of humans. If such a function can be found to be robust and accurate, it would be utilized by industry and academia alike. The power to predict human discomfort based on posture and motion would allow designers to construct products that are more comfortable and safer and that would allow for better performance in vibration environments.

REFERENCES

1. Adams M.A.; Hutton, W.C.; The effect of posture on the lumbar spine. *J. Bone Joint Surg.* **1985,** 67-B, 625-629.

2. Ewing, C.L.; Thomas, D.J. *Human head and neck response to impact acceleration.* Naval Aerospace Medical Research Lab: Pensacola, FL, **1972**.

3. Fard, M.A.; Ishihara, T.; Inooka, H. Transmission of the translational trunk vibration to the head-neck complex. *JSME International Journal*. **2001,** 46, 116-122.

4. Fritz, M. Three-dimensional biomechanical model for simulating the response of the human body to vibration stress. *Med. Biol. Eng. Copmut*. **1998**, 36, 686-692.

5. Mansfield, N.J. *Human response to vibration;* CRC Press: Boca Raton, FL, **2004**.

6. Mansfield N.J.; Holmlund, P.; Lundstrom, R.; Lenzuni, P.; Nataletti, P. Effect of vibration magnitude, vibration spectrum and muscle tension on apparent mass and cross-axis transfer functions during whole body vibration exposure. *J. Biomechanics.* **2006,** 39, 3062-3070.

7. Mansfield, N.J.; Maeda, S. The apparent mass of the seated human exposed to single-axis and multi-axis whole-body vibration. *J. Biomechanics.* **2007**, 40, 2543-2551.

8. Paddan, G.S.; Griffin, M.J. The transmission of translation seat vibration to the head – II. Horizontal seat vibration. *J. Biomechanics.* **1988,** 21, 199-206.

9. Rahmatalla, S.; Xia, T.; Contratto, M.; Kopp, G.; Wilder, D.; Frey Law, L.; Ankrum, J. Three-dimensional motion capture protocol for seated operator in whole body vibration. *Industrial Ergonomics*. **2008,** 38 425-433.

10. Rahmatalla, S.; Xia, T.; Contratto, M.; Wilder, D.; Frey Law, L.; Kopp, G.; Grosland, N. 3D displacement, velocity, and acceleration of seated operators in a whole body vibration environment using optical motion capture systems. In The Ninth International Symposium on the 3-D Analysis of Human Movement, Valenciennes, France, 28-30 June, **2006**.

11. Viviani, P; Berthoz, A. Dynamics of the head-neck system in response to small perturbations. *Biol. Cybernetics.* **1975,** 19, 19-37.

12. Williams, E.J. Experimental designs balanced for the estimation of residual effects of treatments. *Australian Journal of Scientific Research.* **1949,** A2, 149-168.

APPENDIX

Appendix A. Additional Figures

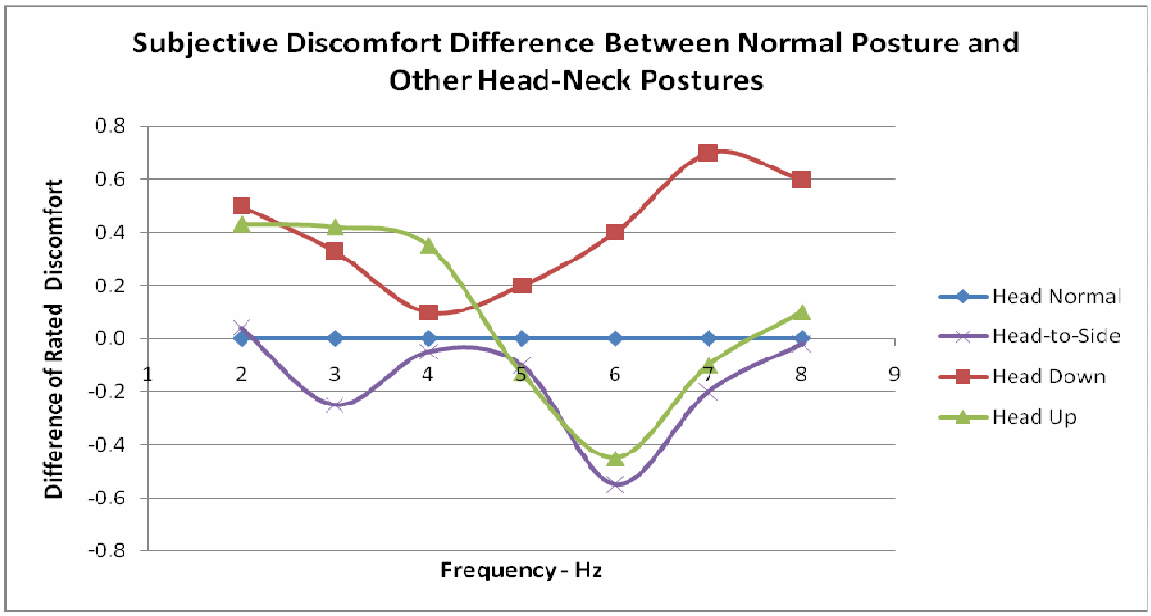

Figure A.1 – Average of difference in subjective reported discomfort between normal posture and each alternative head-neck posture for 10 subjects. Normal posture rating is used as a baseline.

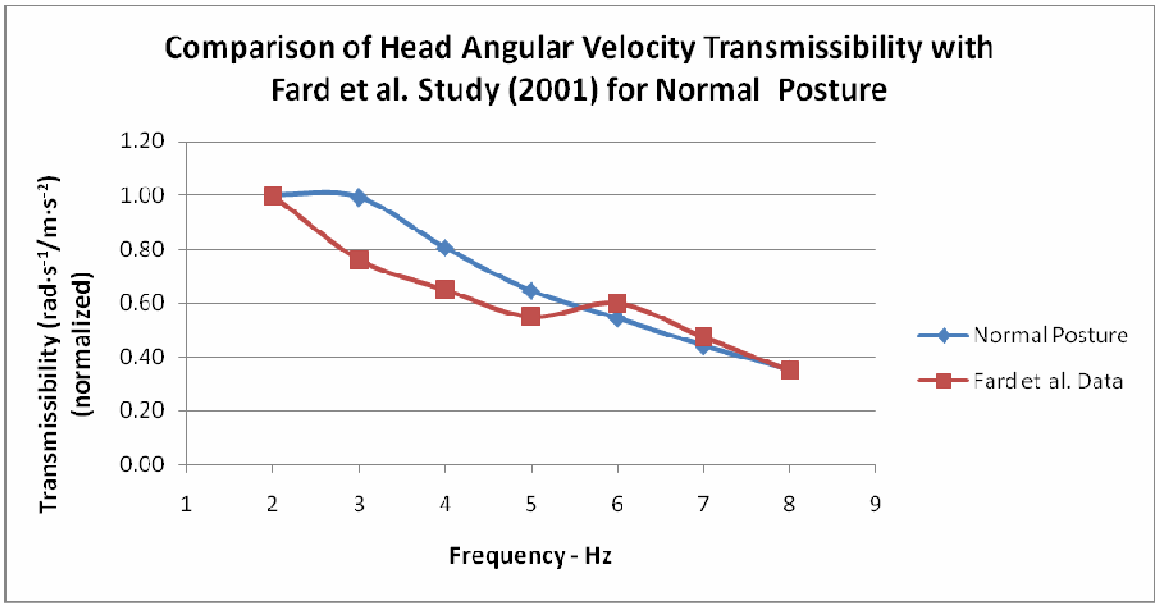

Figure A.2 – Comparison of angular velocity transmissibility from average of 6 subjects from Fard et al. (2001) study in normal posture